Nature Communications

https://doi.org/10.1038/s41467-025-67409-w

Article in Press

Engineering microbial consortia for mixed plastic upcycling

Received: 5 October 2025

Accepted: 27 November 2025

Cite this article as: Diao, J., Tian, Y., Park, S. *et al.* Engineering microbial consortia for mixed plastic upcycling. *Nat Commun* (2025). https://doi.org/10.1038/s41467-025-67409-w

Jinjin Diao, Yuxin Tian, Sunkyu Park, Seong-Min Cho & Tae Seok Moon

Engineering microbial consortia for mixed plastic upcycling

Jinjin Diao[1,2†], Yuxin Tian[1,3†], Sunkyu Park[4], Seong-Min Cho[4*], and Tae Seok Moon[3,5*]

[1] Department of Energy, Environmental and Chemical Engineering, Washington University in St. Louis, St. Louis, MO 63130, USA

[2] Department of Chemical Engineering, Guangdong Technion-Israel Institute of Technology, Shantou, Guangdong 515063, China

[3] Synthetic Biology Group, J. Craig Venter Institute, La Jolla, CA 92037, USA

[4] Department of Forest Biomaterials, North Carolina State University, Raleigh, NC 27695, USA

[5] Moonshot Bio, Inc., North Andover, MA 01845, USA

[†] These two authors contribute equally.

[*]To whom correspondence should be addressed

Tae Seok Moon (lead corresponding author)
Tel: +1 858-200-1800
Email: tsmoon7@gmail.com
J. Craig Venter Institute
4120 Capricorn Lane
La Jolla, CA 92037 USA

Seong-Min Cho
Email: scho26@ncsu.edu
Department of Forest Biomaterials
North Carolina State University
Raleigh, NC 27695 USA

Abstract

Recent studies in developing processes using 'single' plastic waste for microbial conversion have demonstrated great promise in advancing a circular economy. However, chemical complexity and compositional variability of post-consumer 'mixed' plastic waste pose huge challenges to using it as a feedstock for biomanufacturing. Here, we present a process leveraging a synthetic microbial consortium, comprising *Rhodococcus jostii* strain PET and *Acinetobacter baylyi* ADP1, enabled by engineering the division of labor. The robust consortium synergistically and stably consumes diverse mixtures of oxygenated compounds, derived from the depolymerization of post-consumer, mixed plastic waste, regardless of the fluctuating plastic waste compositions. We evaluate the upcycling potential of the stable consortium by applying rational metabolic engineering to both specialists, enabling the funneling of these oxygenates into lycopene and lipids. This work highlights the potential of stable microbial consortia to valorize untapped, mixed plastic waste for sustainable biomanufacturing, offering a promising solution to global plastic pollution.

Introduction

Global plastic demand has driven its annual production from 1.5M metric tons in 1950 to 367M in 2020[1, 2]. However, the current 'take-make-waste' linear plastic system relies on large quantities of fossil resources, contributing to greenhouse gas emissions[3]. Because synthetic polymers are highly recalcitrant to degradation, their increase in production, combined with ineffective end-of-life management, has led to serious global plastic pollution[4-7]. Developing effective plastic recycling or upcycling technologies is urgently needed[8].

Recently, plastic hybrid upcycling, a process that integrates chemical deconstruction with microbial bioconversion, has shown great promise for the rapid depolymerization and highly efficient upcycling of single-stream plastic waste[9-11]. Advanced chemical processes have demonstrated the feasibility of deconstructing mixed plastics without the need for pre-sorting[12-14], offering a promising opportunity to upcycle mixed plastics using biocatalysis. For example, a recent study demonstrated the transition metal-based depolymerization of mixed plastic waste – comprising poly(ethylene terephthalate) (PET), polyethylene (PE), and polystyrene (PS) – into a mixture of oxygenated small molecules that serve as substrates for biological conversion[15]. Nevertheless, this approach requires high temperature and pressure to initiate the reaction, and the leaching of metal sites into the solution adds complexity to downstream processing, as detoxification is needed before subsequent bioconversion. To overcome this limitation, Dou et al. developed an ionic liquid-based method for chemically depolymerizing mixed plastics, with the resulting effluent upgraded biologically without additional separation. However, this approach is restricted to polyester-type plastics such as PET and PLA and does not adequately capture the complexity of real-world, post-consumer mixed plastic waste streams[16]. Consequently, there is an urgent need for an efficient depolymerization method capable of breaking down post-consumer mixed plastic waste into biocompatible compounds, without the need for downstream processing prior to bioconversion.

Current plastic upcycling approaches, centered on employing a single microbial host, have inherent limitations. Specifically, extensive genetic modifications are required to equip the monoculture host with specialized catabolic pathways for utilizing complex substrates without carbon catabolite repression, as well as multiple enzymes and regulators for the biosynthesis of target products. These modifications often impose metabolic burdens on the microbe by disrupting the delicate distributions of the metabolic flux and destabilizing metabolic networks, leading to reduced overall upcycling efficiency[17]. Moreover, the depolymerization of plastics produces effluent streams with batch-to-batch variations in substrate compositions, caused by the inherent variability of post-consumer plastic waste streams. This variation makes the biological conversion less efficient because monoculture hosts are highly susceptible to environmental and nutrient perturbations[18].

In contrast, microbial consortia can have high enzyme diversity and task modularity through the division of labor (DOL), and they have emerged as a promising alternative for bio-manufacturing of valuable chemicals from complex biomass waste[19-21]. The positive interactions between species in microbial consortia, along with the ability to spatially segregate metabolic pathways across specialized strains, enhance their robustness against environmental fluctuations[22]. For instance, microbial consortia derived from enriched environmental inocula were paired with chemical processing to degrade various plastics, including PET[23, 24], high-density polyethylene[25] (HDPE),

and polycarbonate[23]. In another study, efficient microbial consortia were developed from the enrichment of plastic landfill inocula to valorize polyolefin pyrolysis wax into polyhydroxyalkanoates[26]. However, these microbial consortia were developed using a top-down approach, and their complex microbial interactions and a lack of efficient genetic engineering tools make it challenging to manipulate their structure and function or to rewire their metabolic networks for bioproduction. In contrast, the bottom-up approach utilizes well-developed microbial hosts to engineer synthetic microbial consortia, providing unique opportunities to control their composition and function for targeted bioprocesses[19]. While the implementation of DOL enabled the bottom-up engineering of microbial consortia for upcycling a single plastic stream of PET[27], the DOL-based approach remains underexplored for mixed plastic upcycling.

Here, we demonstrate a hybrid, mixed-plastic upcycling process that integrates transition metal-free chemical catalysis with an engineered microbial community to convert post-consumer, mixed plastic waste into valuable chemicals (Figure 1). In the chemical catalytic step, a quintuplet plastic mixture, comprising low-density polyethylene (LDPE), HDPE, polypropylene (PP), PET, and PS, is destructed via oxidative degradation using nitric acid or *p*-toluenesulfonic acid. The resulting effluent containing diverse oxygenates is utilized for bioconversion. To combat the substrate complexity, we construct engineered microbial consortia by leveraging DOL. The robust consortia can completely metabolize diverse mixtures of oxygenates, regardless of the compositional variability of the effluents from post-consumer mixed plastic waste. Notably, the optimized consortium stably maintains its metabolic capability and population balance for at least 21 days. Finally, we develop a process to upcycle real mixed plastic waste into target products, including lycopene and microbial lipids. Overall, this work highlights the potential of engineering DOL to assemble robust and stable microbial consortia capable of overcoming the intrinsic challenges of previous mixed plastic upcycling processes. Furthermore, validating the practicability of using mixed plastics as feedstocks for biomanufacturing lays a foundation for a fully circular plastic economy.

Results

Assembling a microbial consortium comprising two specialists

The variations in monomer and bond types, coupled with the mixed nature of post-consumer waste, necessitate costly separation methods to isolate individual polymers for recycling[28]. Chemical processes of deconstructing mixed plastics into metabolizable substrates open up new opportunities for upcycling commingled plastics through bioconversion[29]. We aim to convert mixed plastic waste into feedstocks through oxidative degradation, followed by a biological valorization process (Figure 1). Previous studies demonstrated oxidative degradation under harsh conditions for deconstructing polyolefins to produce oxygenated compounds[30-33]. These studies prompted us to explore oxidative degradation under milder conditions in upcycling post-consumer mixed plastic waste.

We adapted the oxidation process by substituting nitric acid for the high-pressure oxygen gas and lowering the temperature to 180°C. Additionally, carbon conversion efficiency or simply carbon efficiency – defined as the ratio of moles of carbon in the resulting compounds relative to that in the starting plastic – was assessed to compare the effectiveness of the degradation process across

different single-component post-consumer plastics, including a LDPE zip bag, an HDPE bottle, a PP cup lid, a PET bottle, and a PS Styrofoam™ cup (Supplementary Figure 1). The destruction of LDPE and HDPE yielded acetic acid (AA) and C_4 to C_7 dicarboxylic acids (DCAs), including succinic acid, glutaric acid, adipic acid, and pimelic acid, as reported in a previous study[34], with carbon efficiencies of 35.1% and 39.0%, respectively. PP was converted into AA and lactic acid (LA) with a carbon efficiency of 25.4%. While a previous study reported that oxidative destruction of post-consumer PET produced AA[33], our process resulted in a yield of 71.6% terephthalic acid (TPA) (Supplementary Figure 2 and Supplementary Table 1).

Similarly, the PS destruction through the adapted oxidative process yielded 4-nitrobenzoic acid[30]. However, there are a limited number of industrially relevant microbes capable of catabolizing 4-nitrobenzoic acid, rendering it incompatible with microbial conversion processes. A chemical process involving selective, acid-catalyzed, aerobic oxidation under visible light has been developed to deconstruct PS into benzoic acid (BEN), a compound readily metabolized by various microbes[35]. Consequently, we adopted this method for PS deconstruction. This process yielded BEN with a carbon efficiency of 39.6% (Supplementary Figure 2 and Supplementary Table 1), nearly identical to the level reported previously[35].

Next, a quaternary plastic mixture consisting of LDPE, HDPE, PP, and PET was subjected to oxidative degradation. Although the HDPE degradation favors a longer reaction time (180°C for 8 h) compared to that of LDPE (180°C for 6 h), we identified conditions capable of effectively deconstructing the plastic mixture. Treating the post-consumer mixed plastic waste at 180°C for 8 h increased the degradation efficiency of PE (45.2%) but resulted in moderately decreased TPA yields (67.8%) compared to those observed from the destruction of the corresponding individual plastics (Supplementary Figures 2-3 and Supplementary Tables 1-2).

Although our previous study revealed that *Rhodococcus jostii* strain PET (RPET) can simultaneously consume both TPA and ethylene glycol (EG) derived from post-consumer PET[36], its ability to utilize aliphatic carboxylic acids remains unexplored. Consequently, we tested RPET for growth in minimal medium supplemented with AA, LA, or C_4 to C_7 DCA as the sole carbon source (Figure 2a). RPET completely metabolized individual compound (Figure. 2b); however, when the mixture (0.5 g/L each) was used, large amounts of glutaric (C5), adipic (C6), and pimelic (C7) acids remained unconsumed (Figure 2c). Thus, RPET alone may be ineffective for mixed plastic upcycling.

Synthetic microbial consortia have emerged for various applications, as they are believed to be superior to single strains due to the diversion of labor (DOL)[37, 38]. Since RPET was validated as a specialist for aromatic carboxylic acids[36, 39], we sought to select a specialist efficiently consuming aliphatic carboxylic acids. The soil bacterium *Acinetobacter baylyi* ADP1 is notable for its ability to utilize saturated dicarboxylic acids for aerobic growth[40]. To confirm its efficacy for utilizing aliphatic carboxylic acids, we used the same set of individual compounds and their mixtures as sole carbon sources. As expected, *A. baylyi* ADP1 completely metabolized individual compound (Figure 2d). Additionally, only a small fraction of pimelic acid remained unconsumed when the mixture was used (Figure 2e). Furthermore, under mixed substrate conditions, ADP1 consumed 97% of the aliphatic carboxylic acids, while 81% consumption was observed for RPET (Figure 2f). These results suggest that ADP1 can be an ideal aliphatic carboxylic acid specialist for assembling a consortium for mixed plastic upcycling.

We assembled microbial consortia (Figure 2g), which we termed specialist RPET (SR) and specialist ADP1 (SA)-based microbial consortia (RAMC). To test consortia, we inoculated SR, SA, or RAMC (initial OD_{600} = 0.2; RAMC with a ratio of 1:1) into minimal medium containing simulated, mixed plastic deconstruction products (125 mM carbon in total) as the carbon source and 1 g/L ammonium sulfate as the nitrogen source. SR completely consumed the aromatic carboxylic acids (TPA and BEN) but showed a limited utilization of aliphatic carboxylic acids (Figure 2h and Supplementary Figure 4). Notably, a significant overflow of succinic acid was observed in the SR monoculture. SA specialized in consuming aliphatic carboxylic acids but failed to metabolize TPA. Distinct from either monoculture, RAMC completely consumed all the substrates (Figures 2h, i), highlighting the potential of this DOL design for mixed plastic upcycling.

Modulating the performance of RAMC

Next, we systematically examined the substrate consumption of RAMC across media with total carbon concentrations ranging from 125 mM to 750 mM by modulating the initial cell density ratios of SR to SA as 9:1, 7:3, 5:5, 3:7, and 1:9 (Figure 3a). RAMC with ratios of 9:1, 7:3, 5:5, and 3:7 achieved complete substrate consumption when the total carbon concentration was below 500 mM (Figure 3b and Supplementary Figures 5-8). At higher concentrations (625 and 750 mM), RAMC's performance decreased, likely due to increased osmotic stress caused by NaOH-mediated medium neutralization (Supplementary Figures 9, 10). An examination of individual substrate consumption profiles revealed that increasing the relative cell density of SR resulted in a monotonic increase in TPA consumption by RAMC, particularly at high carbon concentrations (Supplementary Figures 8-10). A similar trend was observed for glutaric acid (C5) consumption by RAMC at 625 mM and 750 mM, where increasing the relative cell density of SA led to a monotonic improvement of glutaric acid degradation (Supplementary Figures 9, 10). As the total carbon concentration increased from 125 to 375 mM, cell biomass accumulation of RAMC with ratios of 9:1, 7:3, 5:5, and 3:7 increased monotonically, but no significant differences were observed between these consortia (Figure 3c).

RAMC with varying initial compositions were grown in minimal medium supplemented with 10- or 20-fold diluted effluent streams from the deconstruction of individual post-consumer plastic streams, including LDPE, HDPE, and PP (Figure 3d). Additionally, 10 mM TPA and BEN (in 10-fold diluted medium) or 5 mM of each (in 20-fold diluted medium), derived from post-consumer PET and PS, respectively, were supplied (Figure 3d). A HPLC assay revealed that the 10- and 20-fold diluted media had carbon levels nearly similar to those of media with 250 mM and 125 mM carbon concentrations of simulated, mixed plastic deconstruction products, respectively (Supplementary Figure 11).

In all cases, RAMC outperformed both specialist monocultures in consuming the oxygenated compounds, regardless of the initial compositional ratios (Figure 3e), consistent with our findings using the simulated media (Figure 3b). Biomass accumulation of monoculture was significantly lower under real-plastic conditions compared with the simulated conditions (Figure 3c, e). This reduction is likely due to the toxic effects of additives present in real plastic waste. While RAMC almost completely consumed the oxygenates in both media (Figure 3e and Supplementary Figures 12, 13), biomass accumulation was lower in the 10-fold diluted medium than in the medium with 250 mM carbon from simulated products, except for RAMC with the ratio of 9:1 (Figure 3c, e). Notably, increasing the relative initial cell density of SR in RAMC improved the final biomass accumulation to some extent (Figure 3e).

Sensitivity analysis of RAMC performance in response to variations in post-consumer mixed plastic composition

We performed a sensitivity analysis to evaluate the robustness of RAMC in degrading oxygenated compounds derived from mixed plastics in varying compositions. We defined a minimal medium supplemented with simulated products, including AA, LA, C_4 to C_7 DCAs, TPA, and BEN at a total carbon concentration of 250 mM, as the basic synthetic medium (SM). To mimic the variability of post-consumer mixed plastic waste, we adjusted the carbon concentration of each compound in the simulated products, varying the additional carbon (AC) content from 40 mM to 160 mM (Figure 4a).

RAMC maintained a 100% total consumption rate, even when the AC from TPA (mimicking PET variability) was increased to 160 mM (Figure 4a and Supplementary Figures 14-16). However, the performance of RAMC declined with increasing BEN (mimicking PS variability), AA+C_4 to C_7 DCAs (PE variability), or AA+LA (PP variability) (Figure 4a and Supplementary Figures 17-25). Notably, RAMC with a ratio of 9:1 (hereafter, RAMC_9/1) exhibited strong tolerance to these variations, maintaining consumption rates above 90% even when the AC was increased to 160 mM. Interestingly, with increasing AC derived from PE or PP, a higher initial density of SR improved TPA consumption (Supplementary Figure 20-25), suggesting the presence of an unidentified mechanism impacting the catabolism of TPA and aliphatic carboxylic acids in RAMC. However, this effect was not observed for BEN consumption (Supplementary Figures 17-19).

Biomass accumulation was used to evaluate the performance of RAMC in response to the variability of post-consumer mixed plastic waste. For this purpose, linear regression analysis was employed to determine the relationship between biomass accumulation and carbon source concentration. Increasing the AC derived from TPA linearly increased biomass accumulation, regardless of the initial cell density ratios (Supplementary Figure 26). However, under BEN and AA+C_4 to C_7 DCAs conditions, only RAMC_9/1 showed a significant linear increase (Supplementary Figures 27, 28). In the AA+LA condition, RAMC with ratios of 9:1 and 7:3 exhibited nearly identical slopes (Supplementary Figure 29). Among the four conditions tested, the TPA-biomass linear equation for RAMC_9/1 had the steepest slope (Table 1), implying that the abundance of PET in post-consumer, mixed plastic waste streams may play a critical role in determining the carbon-to-biomass conversion efficiency of RAMC.

To further gauge the potential of RAMC_9/1, simulated, mixed plastic deconstruction products were replaced with real plastic deconstruction products. RAMC_9/1 was grown in the minimal medium supplemented with 10-fold diluted, real plastic deconstruction products as the sole carbon source (RM; see Methods for preparation details), along with an additional 5 mM or 10 mM TPA (derived from post-consumer PET) to mimic the excess PET in post-consumer mixed plastic waste (Figure 4b, c). RAMC_9/1 nearly completely consumed all the resultant oxygenated compounds (Figure 4c, Supplementary Figure 30). Increasing the TPA concentration improved biomass accumulation, following the linear TPA-biomass relationship predicted using data from the simulant experiment (Figure 4d and Supplementary Figure 26). Similarly, when RAMC_9/1 was examined in RM with additional BEN (from post-consumer PS), the changes in its biomass accumulation also followed the linear BEN-biomass relationship (Supplementary Figures 27, 31). However, increasing the liquid effluents from PE or PP deconstruction in RM was detrimental to cell growth, preventing the corresponding sensitivity tests. Collectively, our results demonstrate that RAMC_9/1 is the optimal choice for efficient valorization of mixed plastics. Nonetheless,

further sensitivity analyses of PE and PP under real conditions are necessary to evaluate their impact on RAMC_9/1 performance.

Engineering RAMC for upcycling post-consumer mixed plastic waste into lycopene and lipids

Biological valorization offers significant potential when paired with chemical pretreatment processes for efficient conversion of complex solid wastes into useful compounds[36, 41, 42]. To achieve mixed plastic upcycling, we engineered RAMC by integrating the specific metabolic pathways to convert the oxygenates into valuable compounds (Figure 5a). *Rhodococcus* strains are promising candidates for producing compounds with medical and environmental relevance[43]. Since RPET possesses a carotenoid biosynthetic pathway, it has been developed as a host for upcycling PET hydrolysate into lycopene[36]. Moreover, to enhance the overall economic viability of converting post-consumer PET into lipids, systems metabolic engineering was employed to facilitate the development of an RPET platform for co-producing lycopene and lipids[44].

We leveraged our accumulated technologies to heterologously express the mevalonate (MVA) pathway, the key gene in the downstream terpenoid biosynthetic pathway (i.e., *ispA*), and an $NADP^+$-dependent malic enzyme gene, constructing the derivative strain SR-P (Figure 5b). Additionally, ADP1, known for its capability to produce triacylglycerol (TAG), has served as a robust organism in genetic and metabolic studies[45]. To enable lycopene accumulation in SA, three critical genes in the lycopene biosynthetic pathway, including geranylgeranyl diphosphate synthase (*crtE*), phytoene synthase (*crtB*), and phytoene desaturase (*crtI*), were overexpressed using a replicating plasmid in SA[46], building the derivative strain SA-P (Figure 5b).

SR-P and SA-P were each cultivated in minimal medium supplemented with effluent from post-consumer mixed plastic deconstruction, defined as basal medium (BM) (see Methods for preparation details). The consumption profile of each compound by SR-P was nearly identical to that of SR, except succinic acid (Supplementary Figures 13, 32a). However, a large amount of LA remained unconsumed in SA-P (Supplementary Figure 32a). We speculate that this reduction can be attributed to the metabolic burden imposed by maintaining the large replicating plasmid in SA-P (Figure 5b). Next, we assembled a co-culture of SR-P and SA-P, referred to as RAMC-P, which was cultivated in BM. RAMC-P with ratios of 9:1, 7:3, 5:5, and 3:7 demonstrated nearly 100% consumption of individual compounds except for LA (Supplementary Figure 32a, b). Additionally, RAMC-P with a ratio of 9:1 (hereafter, RAMC-P_9/1) exhibited a slight but significant increase in biomass accumulation (Supplementary Figure 32c), motivating its subsequent application in upcycling mixed plastic wastes into lycopene and lipids.

We further characterized the population dynamics of RAMC-P_9/1 cultivated in BM. Cell counts revealed minimal cell growth of SR-P during the first 36 h of cultivation, followed by a marked increase beginning at 48 h, which is consistent with the TPA consumption profile (Supplementary Figures 33, 34). Meanwhile, a rapid depletion of aliphatic carboxylic acids was observed within the first 36 h of incubation, accompanied by a corresponding increase in SA-P cell density. In addition, a balanced population was achieved after 72 h of cultivation (Supplementary Figure 33b). These results indicate the clear differentiation between the specialists, supporting functional complementarity within RAMC-P: a metabolic arrangement that promotes the division of labor, enhances resistance to environmental perturbations, and contributes to a more stable and balanced community.

When cultivated in BM, RAMC-P_9/1 produced approximately 1248 μg/L of lycopene and 0.37 g/L of total lipids (Figure 5c). Considering the variability of post-consumer mixed plastic waste, the sensitivity analysis of chemical productions was applied to RAMC-P_9/1. For the PET and PS scenarios, since their corresponding deconstructed products are solid, an additional 10 mM of TPA or 11.4 mM of BEN were added to the BM to mimic the varied abundance of these two plastics (both TPA and BEN were derived from the corresponding post-consumer plastic). These additions led to significantly more lycopene and lipid production in RAMC-P_9/1 (1248 ± 56.3 μg/L lycopene and 0.37 ± 0.04 g/L lipids in BM; 1550 ± 56.3 μg/L lycopene and 0.64 ± 0.12 g/L lipids in BM+10 mM TPA; 1436 ± 48.0 μg/L lycopene and 0.48 ± 0.08 g/L lipids in BM+11.4 mM BEN) (Figure 5c). Aside from the previously observed incomplete utilization of LA, a significant amount of glutaric acid remained unconsumed when additional BEN was added (Supplementary Figure 35). The same phenomenon was observed when RAMC_9/1 was cultivated in effluent from real plastics, but not in the simulated media (Supplementary Figures 18, 19, and 30b). This difference indicates that the glutaric acid degradation pathway in these two specialists may be sensitive to some unknown compounds in the real plastic deconstruction products (e.g., plasticizers).

Varying ratios of PE and PP in the initial, post-consumer, mixed plastic waste were also employed to mimic the variability of these plastics (Supplementary Figure 36 and Supplementary Table 2). Similar to the result from the BM medium, incomplete consumption of LA was also observed under these conditions (Supplementary Figure 37). Furthermore, the production levels of lycopene and lipids in RAMC-P_9/1 were not significantly changed when cultivated in these media (lycopene up to 1.7 mg/L and lipids up to 0.48 g/L) (Figure 5d). Together, these results further confirm that RAMC is a robust and promising platform for sustainable biomanufacturing using post-consumer mixed plastic waste that has fluctuating compositions.

Discussion

Global plastic production has been steadily rising, exceeding 400M tons produced annually[36]. Notably, the heterogeneity of the plastic waste stream poses significant challenges in its end-of-life management, rendering the recycling of mixed plastics technically complex and economically inefficient[47]. Here, we developed an upcycling strategy to convert post-consumer mixed plastic waste to value-added chemicals by pairing chemical and biological catalysis. In this process, we established an efficient, transition metal-free oxidative depolymerization method for mixed plastic waste to generate a diverse range of biocompatible oxygenates. Furthermore, by leveraging the principle of DOL, we constructed a synthetic co-culture platform to efficiently upcycle those oxygenates into lycopene and lipids (see Supplementary Tables 3 and 4 for other processes using alternative feedstocks). Altogether, this work exemplifies the promising potential of synthetic microbial consortia for mixed plastic upcycling.

Transition metal-based catalysts have been widely employed in plastic depolymerization[48-50]. Sullivan et al. demonstrated a chemical process that employed Co(II) and Mn(II) co-catalysts for the oxidation of a plastic mixture consisting of PS, HDPE, and PET, which produced BEN, DCAs (C_4-C_{22}), and TPA[15]. Despite its promising efficiency, the utilization of such metal-based catalysts remains challenging. For instance, leaching of metallic sites into the solution increases downstream processing complexity and poses potential toxicity to microbes employed in the bioprocess. In our study, a transition metal-free degradation process was adopted to deconstruct a

plastic mixture consisting of LDPE, HDPE, PP, PS, and PET. While the depolymerization of PS to BEN required a distinct oxidative process, advances in technologies to separate PS from a mixed plastic stream open the door to applications of this transition metal-free, oxidative degradation process[51, 52]. Moreover, further studies focused on engineering potent microbes capable of efficiently catabolizing 4-nitrobenzoic acid could pave the way for a one-step oxidative degradation of mixed plastic waste without the need for PS pre-sorting.

The compositional variations in mixed plastic waste necessitate the rational selection and reprogramming of microbes. For example, Sullivan et al. employed extensive genetic engineering modifications to develop *Pseudomonas putida* KT2440 strains into a platform capable of degrading diverse oxygenates[15]. Notably, individual DCA in the fermentation medium was below 0.1 g/L (except for succinic acid), suggesting that this single-strain platform presumably has a limited capacity to utilize DCA mixtures, particularly at higher concentrations. In general, the total DCA concentration in our medium was 2.3- to 5.0-fold higher than that in Sullivan's medium. Meanwhile, RAMC's consumption of diverse oxygenates at varying concentrations (Figure 3) highlights that DOL can effectively maximize complex substrate utilization without extensive genetic engineering. A closer examination of the odd-chain dicarboxylic acid consumption profiles revealed a clear synergistic effect in the RAMC system, particularly at high DCA concentrations (Supplementary Figures 6-10 and 20-25). In addition, a significant accumulation of succinic acid was observed in the SR monoculture, whereas no such accumulation occurred upon the addition of the SA specialist (Figure 2h, Supplementary Figures 4-10 and 12-25), suggesting a potential cross-feeding relationship at the succinate node between the two specialist strains in the RAMC system. These findings warrant further investigations of interactions within the RAMC system using multi-omics and/or isotopic labeling analysis to inform future efforts in engineering RAMC.

A consistent, quality-controlled supply of feedstocks is essential for biomanufacturing. For example, each biomass must undergo rigorous quality control to ensure uniformity, safety, and efficacy before its biochemical conversion into biofuels[53]. Quality control can be streamlined through real-time analysis, advanced sensors, and artificial intelligence (AI)-based predictive analytics, and active research in this area can reduce costs and processing time. However, these technologies are not yet universally accessible or affordable[54]. In this study, the synthetic microbial consortium demonstrated the capacity to degrade diverse oxygenates in effluents from real mixed plastic waste to produce lycopene and lipids, regardless of fluctuations in plastic compositions (Figure 5). This adaptability marks a promising approach to circumventing the need for stringent feedstock quality control. Moreover, the long-term stability of the RAMC system was tested in the minimal medium supplemented with post-consumer mixed plastic deconstruction products. The results showed that both substrate consumption ability and population balance remained unchanged after 21 days of serial subculture (Supplementary Figure 38). Altogether, our results demonstrate the stability of RAMC, strengthening its practicability.

Metabolically cooperative communities have been shown to increase robustness against environmental perturbations[55]. In our study, prior insights into the metabolic characteristics of both specialists enabled us to develop RAMC by leveraging a bottom-up approach[36, 46, 56], validating RAMC's practicability for degrading complex and compositionally variable feedstocks derived from mixed plastic depolymerization (Figures 3-5). Although the lycopene production in our study is modest compared to the level reported by using microbial fermentation with conventional feedstocks (approximately 2-3 g/L)[57], the obtained level remains comparable to previously reported values using alternative feedstocks (Supplementary Table 3). In addition, our RAMC

system produces microbial lipids under nitrogen-replete conditions, achieving a final lipid content of approximately 26.3% of dry cell weight, 32-fold higher than the PHA yield reported in Sullivan's research[15]. Furthermore, the lipid content level in our study is comparable to industrial levels achieved through microbial batch fermentations, where the lipid content typically ranges from 17% to 70%[58].

Despite these advances, significant challenges remain in optimizing the RAMC system's capacity to upcycle post-consumer mixed plastic waste in an economically feasible manner. First, the degradation pathways for aliphatic carboxylic acids have yet to be fully elucidated. While our comparative genomic analysis has identified several key enzymes involved in the proposed pathways (Supplementary Figure 39), their detailed mapping is essential for developing rational metabolic engineering strategies to reinforce cofactor and redox supply, thereby enhancing productions of target chemicals[59]. Second, since both SR and SA specialists are oleaginous microorganisms, their fatty-acid biosynthetic pathways are strong sinks that divert acetyl-CoA away from heterologous metabolic pathways, reducing the target chemical production. Strategies such as dynamically regulating the carbon flux through endogenous fatty acid biosynthetic and heterologous metabolic pathways could help balance the carbon distribution[60]. However, a limited number of high-throughput strain engineering tools and robust biosensors for developing genetic circuits in these two non-model chassis significantly constrain the application of dynamic regulation to optimize RAMC for enhanced production of target chemicals. Third, our research demonstrates the feasibility of the RAMC system in producing target chemicals through submerged fermentation, the most common industrial approach for biomanufacturing, typically operated in fed-batch or continuous modes, where nutrient and oxygen are optimally distributed and parameters such as pH and temperature are precisely controlled to maximize yields[61]. However, fed-batch fermentation using oxygenates derived from mixed plastic depolymerization has not yet been validated. These challenges will be addressed through ongoing advances in multi-omics analysis, community flux analysis, metabolic modeling, metabolic engineering, the development of synthetic biology tools, and process control.

In summary, this study advances the paradigm of mixed plastic upcycling toward practical deployment by integrating a transition metal-free deconstruction strategy and a robust two-member consortium capable of producing dual products – lipids and lycopene – from various real-world mixed plastic breakdown streams regardless of the plastic compositional variability. Furthermore, given the metabolic versatility of the specialist strains SR and SA, we envision that the RAMC system holds great potential for a wide range of applications, including wastewater treatment, bioremediation, and lignocellulosic valorization.

Methods

Construction of plasmids and strains

DNA was amplified using Phusion High-Fidelity DNA Polymerase (NEB, USA), and all the oligonucleotide primers were synthesized by Integrated DNA Technologies (IDT, USA). DNA fragments were extracted from electrophoresis gels using Zymoclean Gel DNA Recovery Kit (Zymo, USA). Plasmid was assembled via Gibson Assembly (100 mM Tris-HCl, 10 mM $MgCl_2$, 0.2 mM dNTPs, 10 mM DTT, 5% PEG-8000, 1 mM NAD^+, 4 U/μl Taq DNA ligase, 4 U/ml T5 exonuclease, and 25 U/ml Phusion DNA polymerase) method[62]. Correct plasmid assembly was

confirmed by colony PCR, and the sequences of the inserted fragments were verified through Sanger sequencing (GENEWIZ, USA).

The wild type (WT) *Rhodococcus jostii* strain PET (RPET) was from our in-house strain collection, while the WT *Acinetobacter baylyi* ADP1 was purchased from American Type Culture Collection (ATCC identification number: 33305; Manassas, VA). The lycopene and lipid co-producing RPET strain for RAMC-P was from our previous study[44]. The lycopene-producing ADP1 strain was constructed by transforming a self-replicating plasmid (plasmid backbone from Addgene; identification number: 140634; Watertown, MA) expressing three genes involved in the lycopene biosynthetic pathway, including geranylgeranyl diphosphate synthase (*crtE*), phytoene synthase (*crtB*), and phytoene desaturase (*crtI*). The corresponding DNA sequence information is provided in Supplementary Table 5. Genetic engineering of ADP1 was performed following a natural transformation method with modifications[63]. Briefly, a 50 μl aliquot of overnight WT ADP1 culture was added to 5 ml of fresh Luria Broth (LB) media and cultivated at 30°C with shaking at 250 rpm for 3-4 h. Then, a 500 μl sample of the fresh culture in the exponential phase was transferred to a 1.5 ml microcentrifuge tube with transforming plasmid DNA added. This mixture was then incubated at 30°C for 3 h. 200 μl cells were then spread on LB plates with appropriate antibiotics; the plates were incubated at 30°C overnight, or until colonies were visible.

Preparation of simulated minimal media containing model substrates

The simulated, mixed plastic deconstruction products with a total carbon concentration of 750 mM were prepared by adding 30 mM TPA, 30 mM BEN, 33.3 mM acetic acid, 22.2 mM lactic acid, 16.7 mM succinic acid, 13.3 mM glutaric acid, 11.1 mM adipic acid, and 9.5 mM pimelic acid to deionized water, followed by gradual adjustment of pH to 7 using 4 N NaOH. Before microbial cultivation, minimal medium salts were added, and the solution was filtered using 0.22 μm Vacuum Bottle Top Filter (Thermo Fisher, USA). The other simulated minimal media (SM) were prepared by serially diluting the 750 mM medium to the specific carbon concentrations of 125, 250, 375, 500, and 625 mM, or as follows: SM+40 mM AC from PET, 6.51 g/L (294.23 mM carbon); SM+80 mM AC from PET, 7.22 g/L (328.38 mM carbon); SM+160 mM AC from PET, 8.88 g/L (408.38 mM carbon); SM+40 mM AC from PS, 6.35 g/L (292.04 mM carbon); SM+80 mM AC from PS, 7.03 g/L (330.92 mM carbon); SM+160 mM AC from PS, 8.34 g/L (406.21 mM carbon); SM+40 mM AC from PE, 6.85 g/L (297.44 mM carbon); SM+80 mM AC from PE, 7.66 g/L (328.94 mM carbon); SM+160 mM AC from PE, 9.37 g/L (394.19 mM carbon); SM+40 mM AC from PP, 6.80 g/L (291.93 mM carbon); SM+80 mM AC from PP, 8.12 g/L (336.09 mM carbon); SM+160 mM AC from PP, 10.61 g/L (419.00 mM carbon).

Strain cultivation and consortium assembly

If not mentioned otherwise, all the cell cultures were performed in 50 mL glass tubes containing 10 mL minimal salts medium[64], supplemented with 1 g/L ammonium sulfate as the nitrogen source and appropriate carbon sources, as indicated specifically for each experiment. All the seed cultures were prepared using 10 mL minimal salts medium containing 1 g/L glucose as the carbon source. For comparison of aliphatic carboxylic acid consumption capability between specialist strains, WT RPET (SR) and ADP1 (SA) were inoculated (at a final OD_{600} of 0.1) into minimal salts medium containing either 0.5 g/L of each acetic acid, lactic acid, succinic acid, glutaric acid, adipic acid, and pimelic acid, or their mixtures (3.0 g/L in total) as the carbon source. Cell growth of each specialist was measured in a black 96-well plate with a clear bottom (Greiner Bio-one, Austria), using a Tecan Infinite M200 Pro plate reader (Tecan, Switzerland). Abs_{600} (absorbance) values

were converted into OD_{600} values using experimentally determined relationships: $OD_{600} = 1.75 \times Abs_{600}$ for SR and $OD_{600} = 2.22 \times Abs_{600}$ for SA.

For consortium assembly, the corresponding seed cultures were harvested by centrifuging at 3000×*g* for 10 min. The cell pellets were washed twice with sterile deionized water and resuspended to a final OD_{600} of 2. The two cells were then mixed at an initial OD_{600} of 0.2 with cell density ratios of SR to SA set at 9:1, 7:3, 5:5, 3:7, and 1:9. Cultivations were carried out at 30°C with shaking at 250 rpm in a benchtop incubator. Consortium cell growth was monitored by measuring changes in Abs_{600} every 12 h in a black 96-well plate with clear bottom (Greiner Bio-one, Austria) using a Tecan Infinite M200 Pro plate reader (Tecan, Switzerland).

For measuring CFUs, 200 µl of cell culture was harvested and serially diluted to an appropriate cell density. From the selected dilutions, typically those expected to yield 30-300 colonies, 50 µl aliquots were spread onto agar plates. The plates were incubated at 30°C, and colonies were counted once they became visible.

Plastic oxidative depolymerization

Materials

Nitric acid (70%) and *p*-toluenesulfonic acid monohydrate (*p*TsOH·H_2O) were purchased from Fisher Scientific (Waltham, MA). Organic solvents and chemicals, including benzene, acetonitrile, ethyl acetate, n-hexane, sodium hydroxide, hydrochloric acid (37%), and magnesium sulfate, were purchased from Sigma-Aldrich (St. Louis, MO). Plastic waste materials, including an LDPE zip bag, an HDPE bottle, a PP cup lid, a PET bottle, and a PS Styrofoam™ cup, were collected from recycling bins, thoroughly washed, and dried before use, as shown in Supplementary Figure 1.

PS depolymerization

The photo-induced deconstruction of PS was performed under blue LED light irradiation in an oxygen atmosphere provided by O_2 balloons, with slight modifications to a previously reported method[35]. Briefly, clipped PS Styrofoam cup pieces (5.2 g; approximately 50 mmol of PS repeating units) and *p*-TsOH·H_2O (10 mol%, 0.9511 g) were added to a 250-ml Erlenmeyer flask containing 100 mL of benzene/acetonitrile mixture (1:1 by volume). The flask was sealed with a rubber septum and vigorously stirred with a magnetic stir bar until the PS dissolved. Subsequently, the flask was placed in a photo box, where blue LED light (435-445 nm) was irradiated from the side using an Aldrich Micro Photochemical Reactor (Sigma-Aldrich, USA), while blue LED light (460-465 nm) and UVA LED light (390-400 nm) were simultaneously irradiated from the bottom using a 100W LED floodlight purchased from Amazon. The PS depolymerization reaction was carried out at room temperature under light irradiation for 48 hours, during which the initially colorless reaction mixture turned red-brown. Benzoic acid, the final product of this reaction, was extracted through liquid-liquid extraction. Briefly, the reaction solution was alkalized to pH 10 with 0.5 M aqueous NaOH under vigorous stirring. The organic phase was washed twice with 50 ml of water. The resulting aqueous solutions were combined and acidified to pH 2 using 2 M aqueous HCl, followed by three extractions with 100 mL of ethyl acetate each. The combined organic phases were dried over $MgSO_4$ and concentrated *in vacuo*. The resulting crude oily product was washed three times with hot *n*-hexane (50 ml each), and the combined *n*-hexane washes were concentrated *in vacuo*. Finally, the crude residue was purified by trituration with water and dried *in vacuo*, yielding benzoic acid as a white solid.

PET depolymerization

The oxidative PET depolymerization was conducted using nitric acid as the catalyst. Clipped PET bottle pieces (1 g; approximately 5.2 mmol of PET repeating units) and aqueous nitric acid solution (60 ml, 7.2 g of nitric acid/1 g of PET) were added to a 100-ml hydrothermal reactor equipped with a PTFE liner. The reactor was placed in an oven at 180°C for 8 h. After cooling to 4°C, the crude reaction product was filtered. The resulting residue was washed with water and dried *in vacuo*, yielding TPA as a white crystal.

Single-stream PE or PP depolymerization

The oxidative PE or PP depolymerization was conducted using nitric acid as the catalyst. Clipped LDPE zip bag pieces (1 g; approximately 35.7 mmol of PE repeating units), HDPE bottle pieces (1 g; approximately 35.7 mmol of PE repeating units), or PP cup lid fragments (1 g; approximately 23.8 mmol of PP repeating units), and aqueous nitric acid solution (60 ml, 7.2 g of nitric acid/1 g of plastic) were added to a 100-ml hydrothermal reactor equipped with a PTFE liner. The reactor was placed in an oven at 180°C for 6 h or 8 h. After cooling to 4°C, the crude reaction product was filtered. The filtrate was analyzed using high-performance liquid chromatography (HPLC; Agilent Technologies, USA) to determine the composition of the resulting organic acids.

Mixed plastic waste (PET, PE, and PP) depolymerization

The oxidative, mixed plastic waste (PET, PE, and PP) depolymerization was conducted using nitric acid as the catalyst. Clipped LDPE zip bag pieces (0.375 g, 13.4 mmol of PE repeating units), HDPE bottle pieces (0.375 g, 13.4 mmol of PE repeating units), PP cup lid fragments (0.75 g, 17.8 mmol of PP repeating units), and PET bottle pieces (0.5 g, 2.6 mmol of PET repeating units) as well as aqueous nitric acid solution (60 ml, 3.6 g of nitric acid/1 g of plastic; 7.2 g in total) were added to a 100-ml hydrothermal reactor equipped with a PTFE liner. Meanwhile, plastic mixtures with different ratios of each type of single plastic were also employed as starting materials (Supplementary Table 2). The reactor was placed in an oven at 180°C for 8 h. After cooling to 4°C, the crude reaction product was filtered. The filtrate was analyzed using HPLC to determine the composition of the resulting organic acids. The resulting residue was washed with water and dried *in vacuo*, yielding TPA.

Quantification of chemicals

Carboxylic acid was quantified using an Agilent 1260 Infinity II HPLC system equipped with an Aminex HPX-87H ion exclusion column (300 mm × 7.8 mm, particle size 9 mm; Bio-Rad, USA) and a refractive index detector (RID). The column temperature was set at 40°C, and the mobile phase was 0.01 N sulfuric acid, with a flow rate of 1.0 mL/min. The carboxylic acid concentrations were calculated by comparing the peak area values with the specific standard calibration curve with an R^2 coefficient of $\geqslant 0.995$.

Quantification of TPA and BEN was performed using an Agilent 1260 Infinity II HPLC system equipped with an Agilent Poroshell 120 EC-C18 column (4.6 × 100 mm, 2.7 μm) and a UV detector set at 280 nm. The column temperature was set at 60°C, and the flow rate was 1 mL/ min. Mobile phase A (water with 0.1% formic acid) changed to mobile phase B (acetonitrile with 0.1% formic acid) over time as follows (A%/B% with a gradient elution): 92/8 at 0 min, 74/26 at 5 min, 50/50 at 8 min, and 92/8 at 10 min. Concentrations of TPA and BEN were determined by comparing UV absorbance values with the corresponding standard calibration curve for each compound with an R^2 coefficient of $\geqslant 0.995$.

Carbon (or carbon conversion) efficiency, calculated according to the following equation, was used to evaluate the efficiency of plastic depolymerization:

$$Carbon\ efficiency\ of\ PE\ (\%) = \sum Y_i = \sum \frac{W_i/Mw_i}{W_{PE}/(n_i \times Mw_{CH_2})} \times 100 \quad (1)$$

$$Carbon\ efficiency\ of\ PP\ (\%) = Y_{LA} + \frac{2}{3} \cdot Y_{AA} = \frac{W_{LA}/Mw_{LA} + 2W_{AA}/3Mw_{AA}}{W_{PP}/Mw_{PP}} \times 100 \quad (2)$$

$$Carbon\ efficiency\ of\ PET\ (\%) = \frac{8}{10} \cdot Y_{TPA} = \frac{8W_{TPA}/Mw_{TPA}}{10W_{PET}/Mw_{PET}} \times 100 \quad (3)$$

$$Carbon\ efficiency\ of\ PS\ (\%) = \frac{7}{8} \cdot Y_{BEN} = \frac{7W_{BEN}/Mw_{BEN}}{8W_{PS}/Mw_{PS}} \times 100 \quad (4)$$

Here, Y_i is the yield of the produced organic acid *i* (mol%), W_i is the weight of the produced organic acid *i* (g), Mw_i is the molecular weight of the organic acid *i* (g/mol), W_{PE} is the weight of the initial PE (g), n_i is the number of carbon in organic acid *i*, Mw_{CH2} is the molecular weight of the CH_2 unit (g/mol), Y_{LA} is the yield of LA (mol%), Y_{AA} is the yield of AA (mol%), W_{LA} is the weight of the produced LA (g), Mw_{LA} is the molecular weight of LA (g/mol), W_{AA} is the weight of the produced AA (g), Mw_{AA} is the molecular weight of AA (g/mol), W_{PP} is the weight of the initial PP (g), Mw_{PP} is the molecular weight of the PP repeating unit (g/mol), Y_{TPA} is the yield of TPA (mol%), W_{TPA} is the weight of the produced TPA (g), Mw_{TPA} is the molecular weight of TPA (g/mol), W_{PET} is the weight of the initial PET (g), Mw_{PET} is the molecular weight of the PET repeating unit (g/mol), Y_{BEN} is the yield of BEN (mol%), W_{BEN} is the weight of the produced BEN (g), Mw_{BEN} is the molecular weight of BEN (g/mol), W_{PS} is the weight of the initial PS (g), and Mw_{PS} is the molecular weight of the PS repeating unit (g/mol).

Extraction and quantification of lycopene were performed using a modified version of the method described in our previous study[44]. First, 3.5 ml aliquots of cells were centrifuged at 3500×*g* for 10 min and washed with deionized H_2O. After lyophilization, the dry cell pellets were subjected to lycopene extraction using methanol/acetone solution (7:3 v/v) with 0.05% butylated hydroxytoluene (BHT). Lycopene concentration was determined by HPLC, as detailed in our previous study[44]. Briefly, the filtered organic solution with lycopene was analyzed using an Agilent 1260 Infinity II HPLC system equipped with the EC-C18 column and UV detector set at 474 nm. The samples were isocratically eluted for 15 min with a constant flow rate of 1.5 mL/min with the column temperature set at 40°C. The mobile phase consists of a methanol/acetonitrile solution (7:3 v/v). Lycopene concentration in the sample was calculated by comparing the absorbance values with a lycopene calibration curve with an R^2 coefficient of ≥ 0.995.

For lipid extraction and quantification, the lyophilized cell pellets were prepared using the same method as for lycopene extraction and quantification. The dry cell pellet was first ground and resuspended in a conical-bottom glass tube (labeled 'A') with 3 ml of chloroform/methanol solution (2:1 by volume). The tube was then incubated at 37°C with shaking at 250 rpm for 1 h. The organic phase was washed with 1 ml of deionized H_2O and centrifuged at 250×*g* for 10 min. The organic phase was transferred to a new conical-bottom glass tube (labeled 'B'). This extraction cycle was repeated twice. The combined organic phase containing the total lipids was washed twice, first with 1 ml of 1 M KCl and then with 1 ml of deionized H_2O. Finally, the organic phase was transferred into a new glass vial, and the total lipid content was determined by measuring the weight change of the vial after solvent removal.

In the chemical assay experiments, all reagents, including authentic standards, were obtained from Sigma-Aldrich (St. Louis, MO, USA), except for TPA, which was purchased from Alfa Aesar (Ward Hill, MA, USA).

Preparation of media containing real mixed plastic deconstruction products

To prepare RM, 10-fold diluted liquid effluents from the deconstruction of individual plastics, including LDPE, HDPE, and PP, along with 10 mM TPA and BEN derived from post-consumer PET and PS, respectively, were added to minimal salts medium (supplemented with 1 g/L ammonium sulfate) as the carbon source. To prepare BM, 10-fold diluted liquid effluent from mixed plastic (PET, LDPE, HDPE, and PP) deconstruction, along with 10 mM TPA and BEN derived from post-consumer PET and PS, respectively, were added to minimal salts medium (supplemented with 1 g/L ammonium sulfate) as the carbon source.

Dry cell weight measurement

Dry cell weight (DCW) was measured using 2.0 ml microcentrifuge tubes. Cell samples were collected at the end of cultivation and centrifuged at 10,000×*g* for 3 min. The cell pellet was then lyophilized for 12 h, and the DCW (g/L) was calculated by subtracting the weight of the empty tube from the total weight of the tube containing the dried cell pellet.

Statistics & Reproducibility

Unless specified otherwise, all experiments in this study were conducted with three independent biological replicates (N=3) to ensure reproducibility. Statistical analyses were performed using GraphPad Prism (version 10). P-values were determined using independent Student's *t*-tests, with a P-value of less than 0.05 considered statistically significant. Sample size calculations were not performed during the experimental design, and no samples were excluded from the analysis.

Data Availability

Data supporting the findings of this work are available within the main article and its Supplementary Information file. Source data are provided with this paper in the Source Data file.

References

1. Filho, W.L. et al. An assessment of attitudes towards plastics and bioplastics in Europe. *Sci Total Environ* **755**, 142732 (2021).
2. Tiso, T. et al. Towards bio-upcycling of polyethylene terephthalate. *Metab Eng* **66**, 167-178 (2021).
3. Bauer, F. et al. Plastics and climate change-Breaking carbon lock-ins through three mitigation pathways. *One Earth* **5**, 361-376 (2022).
4. Borrelle, S.B. et al. Predicted growth in plastic waste exceeds efforts to mitigate plastic pollution. *Science* **369**, 1515-1518 (2020).
5. Geyer, R., Jambeck, J.R. & Law, K.L. Production, use, and fate of all plastics ever made. *Sci Adv* **3**, e1700782 (2017).
6. Jambeck, J.R. et al. Marine pollution. Plastic waste inputs from land into the ocean. *Science* **347**, 768-771 (2015).
7. Knott, B.C. et al. Characterization and engineering of a two-enzyme system for plastics depolymerization. *Proc Natl Acad Sci U S A* **117**, 25476-25485 (2020).
8. Moon, T.S. Earth: Extinguishing anthropogenic risks through harmonization. *New Biotechnology* **80**, 69-71 (2024).
9. Wei, R. et al. Possibilities and limitations of biotechnological plastic degradation and recycling. *Nat Catal* **3**, 867-871 (2020).
10. Schaerer, L.G. et al. Killing two birds with one stone: chemical and biological upcycling of polyethylene terephthalate plastics into food. *Trends Biotechnol* **41**, 184-196 (2023).
11. Hu, Y., Tian, Y., Zou, C. & Moon, T.S. The current progress of tandem chemical and biological plastic upcycling. *Biotechnology Advances* **77**, 108462 (2024).
12. Ng, K.W.J. et al. A facile alternative strategy of upcycling mixed plastic waste into vitrimers. *Commun Chem* **6**, 158 (2023).
13. Zhang, Z.D. et al. Mixed Plastics Wastes Upcycling with High-Stability Single-Atom Ru Catalyst. *Journal of the American Chemical Society* **145**, 22836-22844 (2023).
14. Zou, C., Chen, J.W., Khan, M.A., Si, G.F. & Chen, C.L. Stapler Strategies for Upcycling Mixed Plastics. *Journal of the American Chemical Society* **146**, 19449-19459 (2024).
15. Sullivan, K.P. et al. Mixed plastics waste valorization through tandem chemical oxidation and biological funneling. *Science* **378**, 207-211 (2022).
16. Dou, C. et al. A hybrid chemical-biological approach can upcycle mixed plastic waste with reduced cost and carbon footprint. *One Earth* **6**, 1576-1590 (2023).
17. Wenk, S., Claassens, N.J. & Lindner, S.N. Synthetic metabolism approaches: A valuable resource for systems biology. *Curr Opin Syst Biol* **30** (2022).
18. Werner, J.J. et al. Bacterial community structures are unique and resilient in full-scale bioenergy systems. *Proc Natl Acad Sci U S A* **108**, 4158-4163 (2011).
19. Lyu, X. et al. Top-down and bottom-up microbiome engineering approaches to enable biomanufacturing from waste biomass. *J Ind Microbiol Biotechnol* **51** (2024).
20. Moon, T.S. SynMADE: synthetic microbiota across diverse ecosystems. *Trends Biotechnol* **40**, 1405-1414 (2022).
21. Moon, T.S. Probiotic and microbiota engineering for practical applications. *Current Opinion in Food Science*, 101130 (2024).

22. Zhou, K., Qiao, K., Edgar, S. & Stephanopoulos, G. Distributing a metabolic pathway among a microbial consortium enhances production of natural products. *Nat Biotechnol* **33**, 377-383 (2015).
23. Putman, L.I. et al. Deconstructed Plastic Substrate Preferences of Microbial Populations from the Natural Environment. *Microbiol Spectr* **11**, e0036223 (2023).
24. Schaerer, L.G. et al. Versatile microbial communities rapidly assimilate ammonium hydroxide-treated plastic waste. *J Ind Microbiol Biotechnol* **50** (2023).
25. Byrne, E. et al. Pyrolysis-Aided Microbial Biodegradation of High-Density Polyethylene Plastic by Environmental Inocula Enrichment Cultures. *Acs Sustain Chem Eng* **10**, 2022-2033 (2022).
26. Lomwongsopon, P., Narancic, T., Wimmer, R. & Varrone, C. Combined thermochemical-biotechnological approach for the valorization of polyolefins into polyhydroxyalkanoates: Development of an integrated bioconversion process by microbial consortia. *Chemosphere* **367**, 143671 (2024).
27. Bao, T., Qian, Y., Xin, Y., Collins, J.J. & Lu, T. Engineering microbial division of labor for plastic upcycling. *Nat Commun* **14**, 5712 (2023).
28. Rahimi, A. & García, J.M. Chemical recycling of waste plastics for new materials production. *Nat Rev Chem* **1** (2017).
29. Ballerstedt, H. et al. MIXed plastics biodegradation and UPcycling using microbial communities: EU Horizon 2020 project MIX-UP started January 2020. *Environ Sci Eur* **33**, 99 (2021).
30. Pifer, A. & Sen, A. Chemical Recycling of Plastics to Useful Organic Compounds by Oxidative Degradation. *Angew Chem Int Ed Engl* **37**, 3306-3308 (1998).
31. Pinsuwan, K., Opaprakasit, P., Petchsuk, A., Dubas, L. & Opaprakasit, M. Chemical recycling of high-density polyethylene (HDPE) wastes by oxidative degradation to dicarboxylic acids and their use as value-added curing agents for acrylate-based materials. *Polym Degrad Stabil* **210** (2023).
32. Bäckström, E., Odelius, K. & Hakkarainen, M. Trash to Treasure: Microwave-Assisted Conversion of Polyethylene to Functional Chemicals. *Ind Eng Chem Res* **56**, 14814-14821 (2017).
33. Anthraper, D., McLaren, J., Baroutian, S., Munir, M.T. & Young, B.R. Hydrothermal deconstruction of municipal solid waste for solid reduction and value production. *J Clean Prod* **201**, 812-819 (2018).
34. Cho, S.M., Chang, H.M. & Park, S. Effects of hydrogen peroxide and sodium nitrate on microwave-assisted polyethylene oxidative degradation in the presence of nitric acid. *Chem Eng J* **499** (2024).
35. Huang, Z. et al. Chemical Recycling of Polystyrene to Valuable Chemicals via Selective Acid-Catalyzed Aerobic Oxidation under Visible Light. *J Am Chem Soc* **144**, 6532-6542 (2022).
36. Diao, J., Hu, Y., Tian, Y., Carr, R. & Moon, T.S. Upcycling of poly(ethylene terephthalate) to produce high-value bio-products. *Cell Rep* **42**, 111908 (2023).
37. Zomorrodi, A.R. & Segre, D. Synthetic Ecology of Microbes: Mathematical Models and Applications. *J Mol Biol* **428**, 837-861 (2016).

38. Shin, J. et al. Compositional and temporal division of labor modulates mixed sugar fermentation by an engineered yeast consortium. *Nat Commun* **15**, 781 (2024).
39. McLeod, M.P. et al. The complete genome of Rhodococcus sp. RHA1 provides insights into a catabolic powerhouse. *Proc Natl Acad Sci U S A* **103**, 15582-15587 (2006).
40. Parke, D., Garcia, M.A. & Ornston, L.N. Cloning and genetic characterization of dca genes required for beta-oxidation of straight-chain dicarboxylic acids in Acinetobacter sp. strain ADP1. *Appl Environ Microbiol* **67**, 4817-4827 (2001).
41. Zhou, X. et al. Valorization of PE plastic waste into lipid cells through tandem catalytic pyrolysis and biological conversion. *Journal of Environmental Chemical Engineering* **11**, 111016 (2023).
42. Rabot, C. et al. Conversion of Polyethylenes into Fungal Secondary Metabolites. *Angew Chem Int Edit* **62** (2023).
43. Cappelletti, M. et al. Biotechnology of Rhodococcus for the production of valuable compounds. *Appl Microbiol Biot* **104**, 8567-8594 (2020).
44. Diao, J., Tian, Y., Hu, Y. & Moon, T.S. Producing multiple chemicals through biological upcycling of waste poly(ethylene terephthalate). *Trends Biotechnol* (2024).
45. Santala, S. et al. Improved triacylglycerol production in Acinetobacter baylyi ADP1 by metabolic engineering. *Microb Cell Fact* **10**, 36 (2011).
46. Biggs, B.W. et al. Development of a genetic toolset for the highly engineerable and metabolically versatile Acinetobacter baylyi ADP1. *Nucleic Acids Res* **48**, 5169-5182 (2020).
47. Kusenberg, M. et al. Opportunities and challenges for the application of post-consumer plastic waste pyrolysis oils as steam cracker feedstocks: To decontaminate or not to decontaminate? *Waste Manag* **138**, 83-115 (2022).
48. Conk, R.J. et al. Catalytic deconstruction of waste polyethylene with ethylene to form propylene. *Science* **377**, 1561-1566 (2022).
49. Celik, G. et al. Upcycling Single-Use Polyethylene into High-Quality Liquid Products. *ACS Cent Sci* **5**, 1795-1803 (2019).
50. Bunescu, A., Lee, S., Li, Q. & Hartwig, J.F. Catalytic Hydroxylation of Polyethylenes. *ACS Cent Sci* **3**, 895-903 (2017).
51. Negari, M.S., Movahed, S.O. & Ahmadpour, A. Separation of polyvinylchloride (PVC), polystyrene (PS) and polyethylene terephthalate (PET) granules using various chemical agents by flotation technique. *Sep Purif Technol* **194**, 368-376 (2018).
52. Nicholas Edward Kob, I., Edn. C08J 11/08//C08L 25:06, 67:02. (ed. W.I.P. Organization) (2002).
53. Li, C.L., Aston, J.E., Lacey, J.A., Thompson, V.S. & Thompson, D.N. Impact of feedstock quality and variation on biochemical and thermochemical conversion. *Renew Sust Energ Rev* **65**, 525-536 (2016).
54. Olawade, D.B. et al. Smart waste management: A paradigm shift enabled by artificial intelligence. *Waste Management Bulletin* (2024).
55. Aulakh, S.K. et al. Spontaneously established syntrophic yeast communities improve bioproduction. *Nat Chem Biol* **19**, 951-961 (2023).

56. Suarez, G.A. et al. Rapid and assured genetic engineering methods applied to Acinetobacter baylyi ADP1 genome streamlining. *Nucleic Acids Res* **48**, 4585-4600 (2020).
57. Liu, X., Ding, W. & Jiang, H. Engineering microbial cell factories for the production of plant natural products: from design principles to industrial-scale production. *Microb Cell Fact* **16**, 125 (2017).
58. Al Azad, S., Madadi, M., Song, G., Sun, C. & Sun, F. New trends in microbial lipid-based biorefinery for fermentative bioenergy production from lignocellulosic biomass. *Biofuel Research Journal* **11**, 2040-2064 (2024).
59. Chen, X., Li, S. & Liu, L. Engineering redox balance through cofactor systems. *Trends in biotechnology* **32**, 337-343 (2014).
60. Tan, S.Z. & Prather, K.L. Dynamic pathway regulation: recent advances and methods of construction. *Curr Opin Chem Biol* **41**, 28-35 (2017).
61. Areniello, M., Matassa, S., Esposito, G. & Lens, P.N. Biowaste upcycling into second-generation microbial protein through mixed-culture fermentation. *Trends in Biotechnology* **41**, 197-213 (2023).
62. Gibson, D.G. et al. Enzymatic assembly of DNA molecules up to several hundred kilobases. *Nature methods* **6**, 343-345 (2009).
63. Biggs, B.W. et al. Development of a genetic toolset for the highly engineerable and metabolically versatile Acinetobacter baylyi ADP1. *Nucleic Acids Research* **48**, 5169-5182 (2020).
64. DeLorenzo, D.M., Henson, W.R. & Moon, T.S. Development of Chemical and Metabolite Sensors for Rhodococcus opacus PD630. *ACS Synth Biol* **6**, 1973-1978 (2017).

Acknowledgments

The authors thank Drs. Fangqiong Ling and Likai Chen for their discussions on this research. The authors also thank James Ballard and Cindy Mittanck for their assistance with editing this manuscript. This work was supported by the U.S. Department of Energy (DE-SC0022003 to T.S.M.), the National Science Foundation (EF-2222403 and OISE-2435184 to T.S.M.), and the American Institute of Chemical Engineers (Langer Prize for Innovation and Entrepreneurial Excellence to T.S.M.). The content is solely the responsibility of the authors and does not necessarily represent the official views of the funding agencies.

Author Contributions Statement

T.S.M. conceived the project. J.D. and T.S.M. designed the study. J.D. and Y.T. performed all the cell cultivation and chemical quantification analyses. S.M.C. and S.P. designed and conducted the plastic depolymerization experiment. All authors wrote and approved the paper.

Competing Interests Statement

T.S.M. has submitted a patent application to the US Patent and Trademark Office related to the aspects of this work involving mixed plastic upcycling through oxidative depolymerization coupled with artificial microbial consortium-driven bioconversion (application number 63/877,807). The remaining authors declare no competing interests.

Table 1. Cell biomass data obtained from the RAMC tests in Figure 4a were subjected to a linear regression analysis to evaluate how changes in carbon source (the independent variable) affected biomass accumulation (the dependent variable). The TPA-biomass equation for RAMC_9/1 exhibited the steepest slope. Details of the equations are provided in Supplementary Figures 26-29.

Source of C	Slope	*P* value
TPA	8.086	<0.0001
BEN	3.574	0.0034
DCA	3.788	0.0013
AA+LA	3.110	0.0008

Figure legends

Figure 1 Schematic diagram of microbial consortium-enabled biotechnology for mixed plastic upcycling. In this work, post-consumer mixed plastic waste was depolymerized into diverse oxygenates through oxidative degradation, using either nitric acid or *p*-toluenesulfonic acid (*p*-TsOH) as catalysts. Subsequently, a robust microbial consortium was developed by leveraging the division of labor to upcycle the diverse oxygenates into lycopene and lipids. The consortium consists of *Rhodococcus jostii* strain PET and *Acinetobacter baylyi* ADP1, with each strain specializing in the degradation of aromatic and aliphatic carboxylic acids, respectively. TCA, tricarboxylic acid cycle. Ph, aromatic ring. *hv*, light irradiation. RT, room temperature. Plastic icons were sourced from BioRender.

Figure 2 Construction of RAMC for the complete degradation of oxygenates. a, Schematic of testing bacterial strains for growth on aliphatic carboxylic acids. **b**, Evaluating RPET's ability to utilize individual acetic acid (AA), lactic acid (LA), succinic acid (C4), glutaric acid (C5), adipic acid (C6), or pimelic acid (C7) as the sole carbon source. Cells were cultivated in minimal medium supplemented with 0.5 g/L of each aliphatic carboxylic acid. **c**, Testing RPET's ability to utilize an aliphatic carboxylic acid mixture as the sole carbon source. Cells were cultivated in minimal medium supplemented with a mixture of aliphatic carboxylic acids (0.5 g/L each; 3 g/L in total). **d**, Evaluation of *A. baylyi* ADP1's ability to utilize individual aliphatic carboxylic acids as the sole carbon source. Cell culture was inoculated into minimal medium supplemented with 0.5 g/L of each aliphatic carboxylic acid. **e**, Testing *A. baylyi* ADP1's ability to utilize an aliphatic carboxylic acid mixture as the sole carbon source. Cells were cultivated in minimal medium supplemented with a mixture of aliphatic carboxylic acids (0.5 g/L each; 3 g/L in total). **f**, Total aliphatic carboxylic acid consumption by RPET and ADP1 tested in **c** and **e**, respectively. **g**, Design and construction of RAMC for degrading a simulated, mixed plastic waste deconstruction product containing aromatic and aliphatic carboxylic acids. **h**, Substrate utilization by RAMC and the two specialist strains grown in the simulated, mixed plastic waste deconstruction product (2.96 g/L; 24.51 mM). Both glucose-grown overnight cell cultures were used as the inoculum. The initial OD_{600} of monocultures and RAMC was set at OD_{600} of 0.2. For RAMC, the initial specialist cell density (OD_{600}) ratio was 1:1. **i**, Total substrate consumption by monoculture strains and RAMC tested in **h**. The consumption of individual substrate is shown in Supplementary Figure 4. For all assays, substrate utilization was determined by HPLC after cultivation. Data represent the mean of three independent experiments (N=3), with error bars depicting the standard deviations from that mean (unpaired two-tailed *t*-test was applied to evaluate significant differences). Source data are provided as a Source Data file.

Figure 3 Optimizing RAMC performance through compositional DOL. a, Schematic of modulating RAMC performance for degrading simulated, mixed plastic waste deconstruction products across various carbon concentrations. The composition of RAMC was modified by adjusting the initial inoculation ratio of the two specialists. **b-c**, RAMC with SR:SA ratios of 9:1, 7:3, 5:5, 3:7, and 1:9 were tested for substrate consumption (**b**) and biomass accumulation (**c**) in media with the total carbon concentrations ranging from 125 to 750 mM (2.88, 5.72, 8.84, 11.25, 14.05, and 16.91 g/L). Despite the compositional variability, the initial OD_{600} of RAMC was maintained at 0.2. The consumption of individual substrates in different growth media is shown in Supplementary Figures 5-10. **d**, Evaluating RAMC performance by using post-consumer plastic deconstruction products. **e**, RAMC with SR:SA ratios of 9:1, 7:3, 5:5, 3:7, and 1:9 were tested for

substrate consumption and biomass accumulation in media supplemented with 20- or 10-fold diluted oxygenate mixtures derived from post-consumer plastic deconstruction. 20-fold, 2.81 g/L (123.97 mM carbon); 10-fold, 5.73 g/L (253.28 mM carbon). The consumption of individual substrate in the two aforementioned media is shown in Supplementary Figures 12-13. In all assays, glucose-grown overnight cell cultures of SR and SA were used as the inoculum, and substrate utilization was measured by HPLC after cultivation. Data represent the mean of three independent experiments (*N*=3), with error bars depicting the standard deviations from that mean (an unpaired two-tailed *t*-test was applied to evaluate significant differences). Source data are provided as a Source Data file. Figure 3a was created with BioRender.

Figure 4 Evaluating RAMC performance in response to the compositional variability of post-consumer mixed plastic waste. a, RAMC with SR:SA ratios of 9:1, 7:3, 5:5, 3:7, and 1:9 were tested for substrate consumption in the basic synthetic medium (SM) supplemented with additional carbons (AC) to simulate plastic compositional variability (TPA for PET, BEN for PS, AA+C4-C7 DCA for PE, and AA+LA for PP). The specific substrate concentration information is provided in Methods. The consumption of each individual substrate in different growth media is shown in Supplementary Figures 14-25. **b**, Ascertaining the trend of RAMC_9/1 data in medium supplemented with real plastic deconstruction products. **c**, RAMC_9/1 was tested for substrate consumption in RM with additional TPA to mimic an excess of PET in post-consumer mixed plastic waste. The consumption of individual substrate in different growth media is shown in Supplementary Figure 30a. Data represent the mean of three independent experiments (*N*=3), with error bars depicting the standard deviations from that mean. An unpaired two-tailed *t*-test was applied to evaluate statistical differences. RM, 5.73 g/L (253.28 mM carbon); RM + 5 mM TPA, 6.40 g/L (284.32 mM carbon); RM + 10 mM TPA, 7.56 g/L (339.57 mM carbon). **d**, Comparison of simulation and experimental results for changes in cell biomass accumulation with increasing TPA concentration. Line, linear regression predictions; dot, experimental data. In all assays, glucose-grown overnight cell cultures of SR and SA were used as the inoculum, and substrate utilization was measured by HPLC after cultivation. Data represent the mean of three independent experiments (*N*=3), with error bars depicting the standard deviations from that mean. Source data are provided as a Source Data file. Figure 4b was created with BioRender.

Figure 5 Upcycling of oxygenates in effluent from post-consumer mixed plastic waste by RAMC. a, The overall process of employing RAMC to upcycle mixed plastic waste into lycopene and lipids. **b**, Engineering metabolic pathways in specialist strains for producing target chemicals. In SR-P, *crtL-b* gene was knocked out via homologous recombination to enable lycopene accumulation. A heterologous mevalonate (MVA) pathway was deployed to rewire intracellular metabolism for enhancing lycopene production. Lipid biosynthesis was decoupled from nitrogen starvation by overexpressing $NADP^+$-dependent malic enzyme (*me*). Gene overexpression in SR-P was achieved using Serine Integrase-based Recombinational Tools (SIRT)-mediated genome editing[44]. In SA-P, three critical genes, geranylgeranyl diphosphate synthase (*crtE*), phytoene synthase (*crtB*), and phytoene desaturase (*crtI*) in the lycopene biosynthetic pathway were overexpressed using a replicating plasmid under the control of an IPTG-inducible promoter. *atoB*, acetyl-CoA C-acetyltransferase; *crtL-b*, lycopene b-cyclase; *HmgS*, hydroxymethylglutaryl-CoA synthase; *HmgR*, hydroxymethylglutaryl-CoA reductase; MK, mevalonate kinase; PMK, phosphomevalonate kinase; PMD, diphosphomevalonate decarboxylase; *idi*, isopentenyl pyrophosphate isomerase; *ispA*, farnesyl diphosphate synthase. **c**, Bioconversion of oxygenates in effluent from post-consumer mixed plastic waste by RAMC-P_9/1. Additional TPA or BEN was

added to evaluate the performance of RAMC-P_9/1 in the target chemical production in response to the variability of post-consumer mixed plastic waste. BM, 5.14 g/L (231.97 mM carbon); BM-T, 7.67 g/L (343.61 mM carbon); BM-B, 7.44 g/L (349.70 mM carbon). **d**, Evaluating the effects of excess PE or PP in post-consumer mixed plastic waste on the upcycling efficiency by RAMC-P_9/1. Post-consumer mixed plastic waste with varying ratios of PE or PP was subjected to depolymerization, and the resulting effluents were applied for subsequent bioconversion. BM PE/PP 3/1, 5.05 g/L (230.05 mM carbon); BM PE/PP 1/3, 4.58 g/L (211.01 mM carbon); BM PE/PP 1/1, 4.70 g/L (214.09 mM carbon). Supplementary Table 2 shows the plastic mixture deconstruction conditions. In all assays, glucose-grown overnight cell cultures of SR-P and SA-P were used as the inoculum. Data represent the mean of three independent experiments, with error bars depicting the standard deviations from that mean. An unpaired two-tailed *t*-test was applied to evaluate statistical differences. Source data are provided as a Source Data file. Figure 5a was created with BioRender.

Editorial summary

The chemical complexity of post-consumer 'mixed' plastic waste limits its use as a feedstock for biomanufacturing. Here the authors combine transition-metal-free plastic deconstruction with a microbial consortium platform to upcycle real-world mixed plastic waste into value-added chemicals.

Peer review information: *Nature Communications* thanks the anonymous, reviewers for their contribution to the peer review of this work. A peer review file is available.

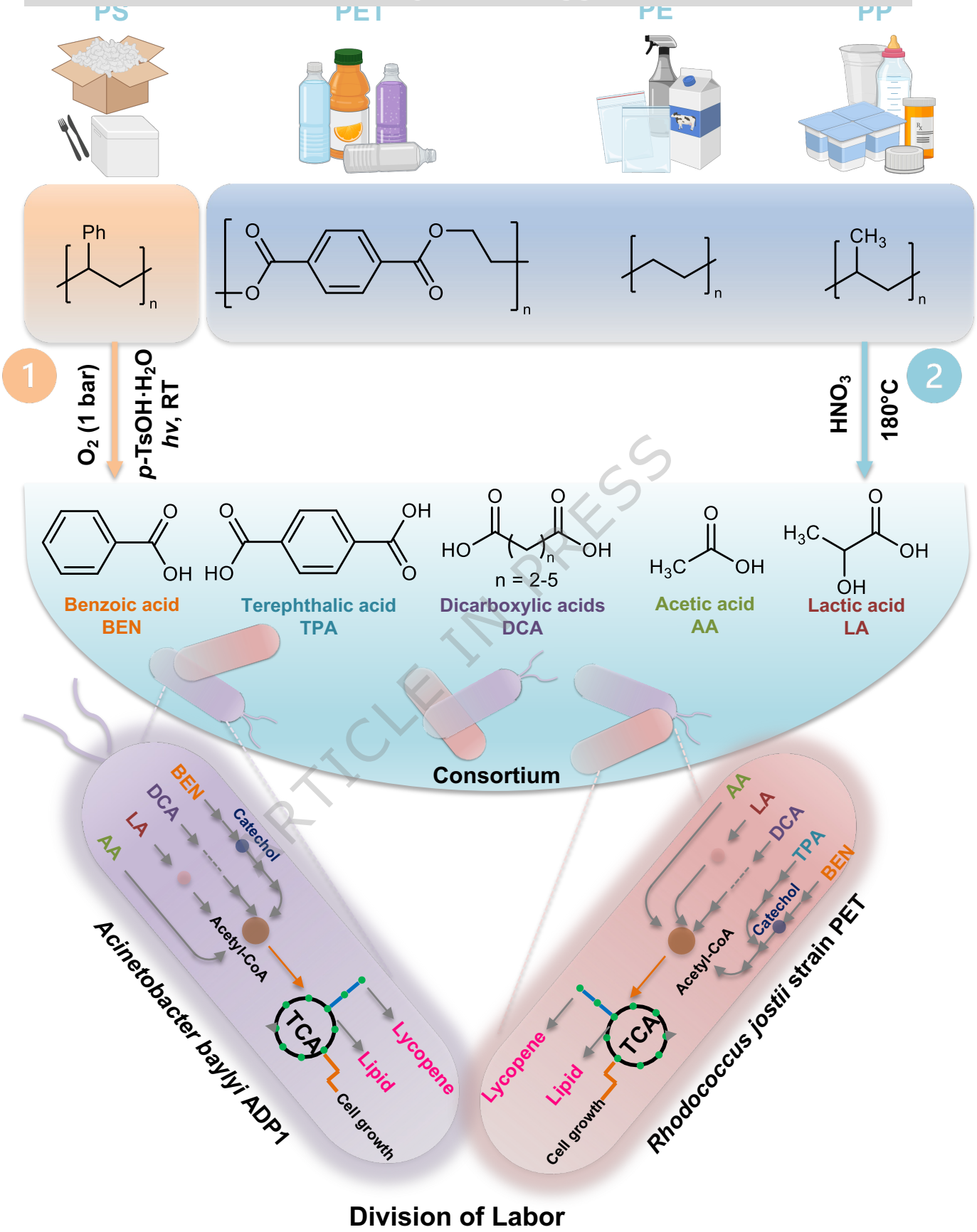

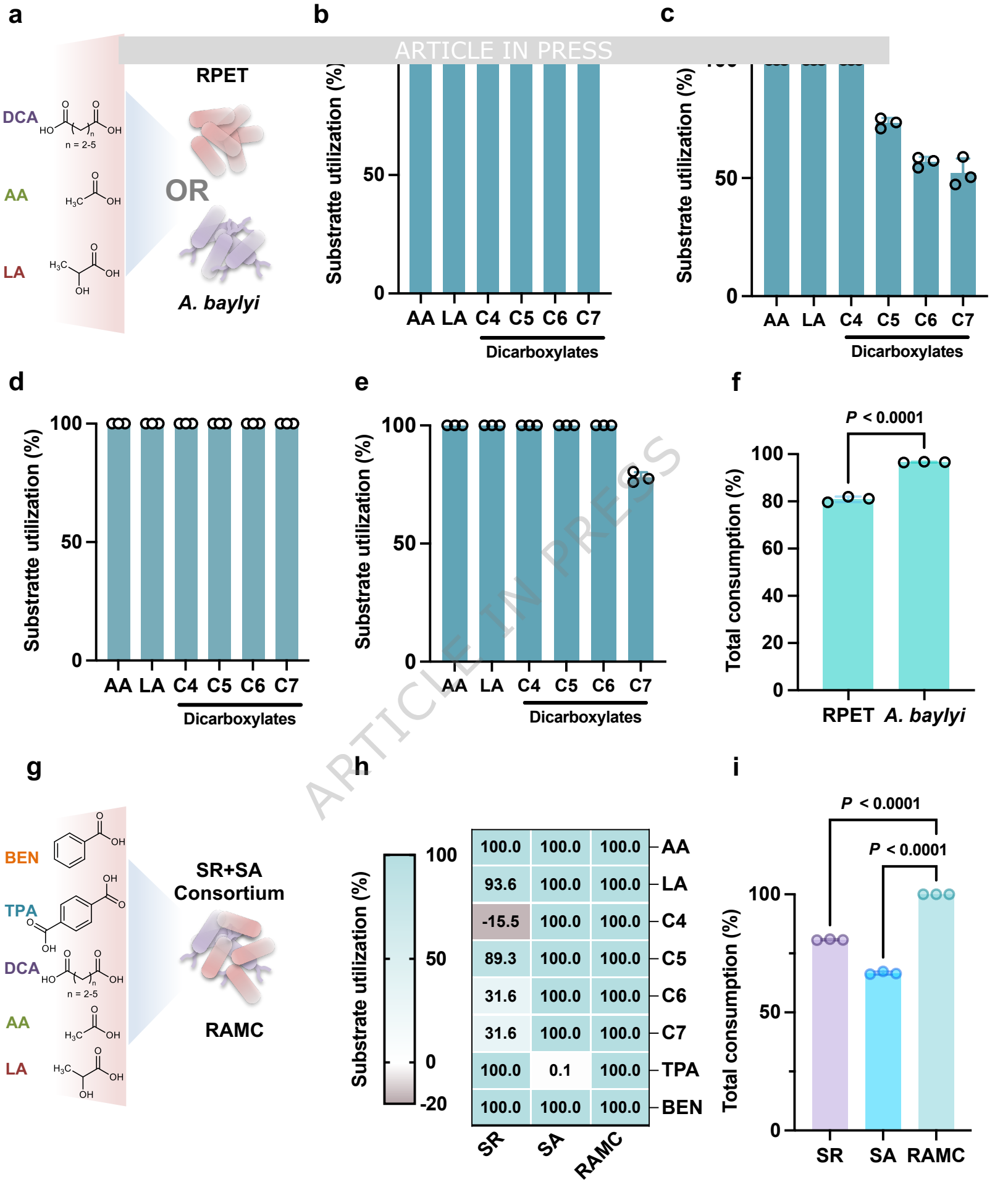

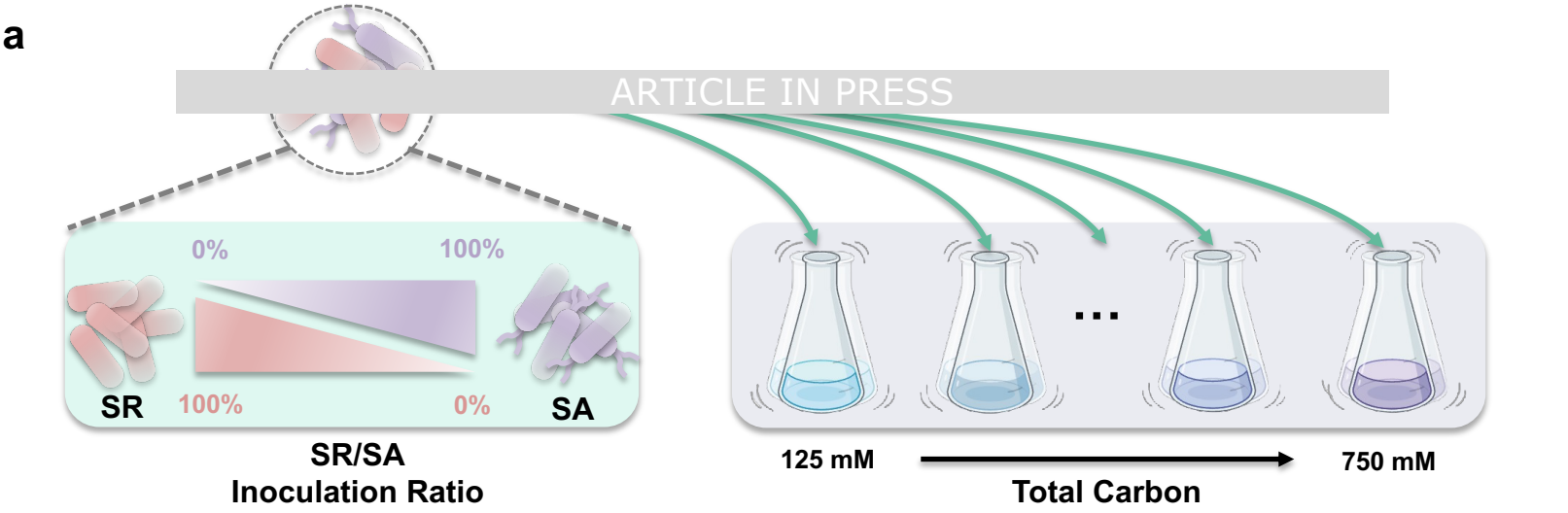

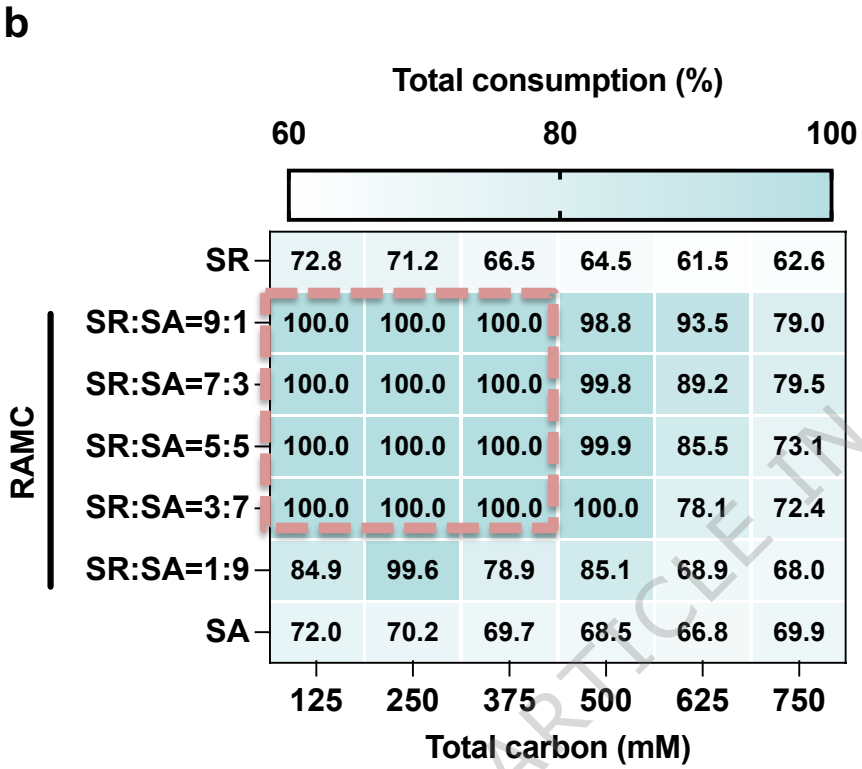

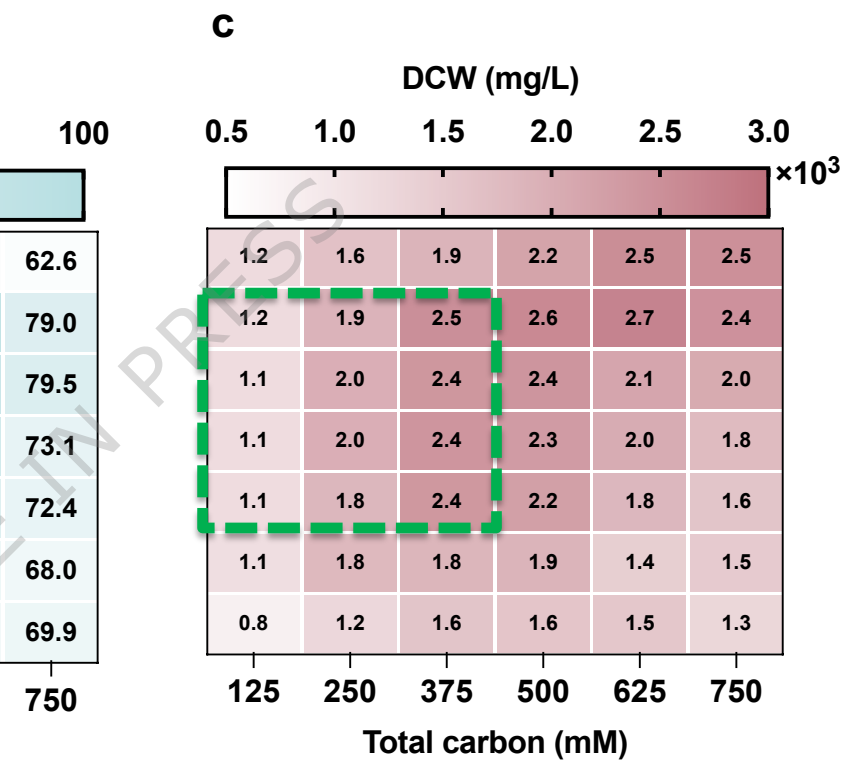

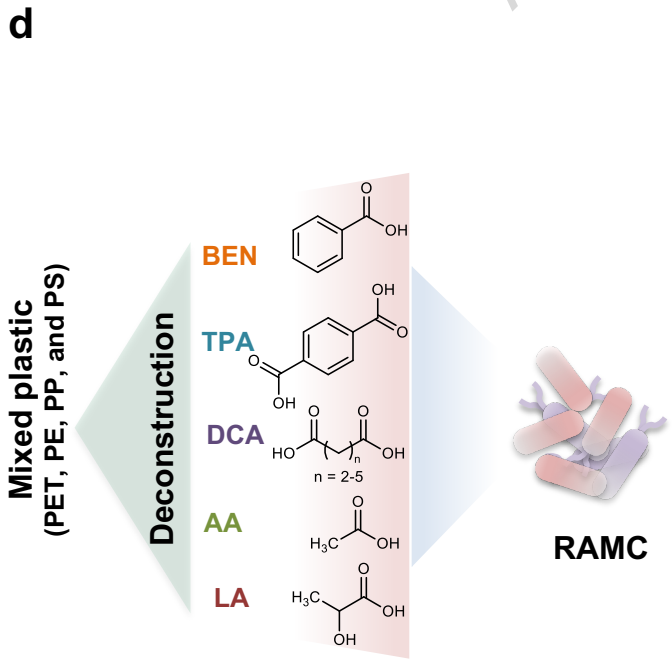

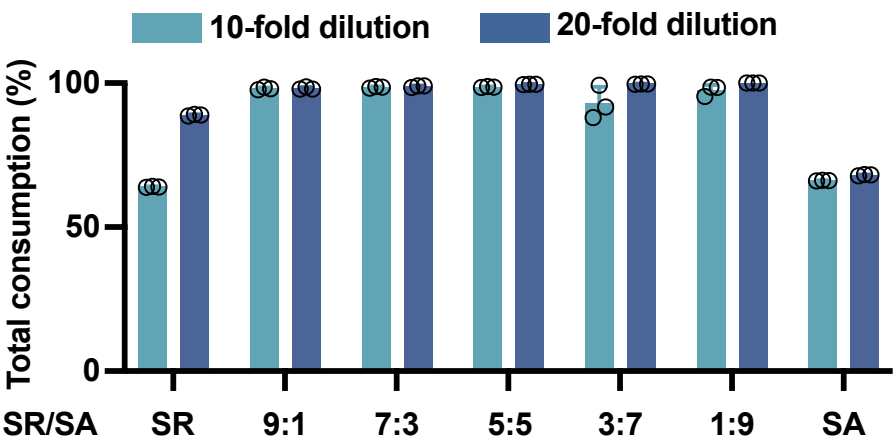

SR/SA	SR	9:1	7:3	5:5	3:7	1:9	SA
Biomass (mg/L)×10³ 10×	0.82 ± 0.10	1.77 ± 0.08	1.43 ± 0.06	1.23 ± 0.28	1.36 ± 0.13	1.43 ± 0.06	0.72 ± 0.08
20×	0.65 ± 0.10	1.18 ± 0.10	1.05 ± 0.30	0.93 ± 0.18	0.87 ± 0.16	0.98 ± 0.23	0.53 ± 0.03

a

	SM+40 mM AC	SM+80 mM AC	SM+160 mM AC	SM+40 mM AC	SM+80 mM AC	SM+160 mM AC	SM+40 mM AC	SM+80 mM AC	SM+160 mM AC	SM+40 mM AC	SM+80 mM AC	SM+160 mM AC
SR:SA=9:1	100.0	100.0	100.0	100.0	100.0	96.5	100.0	100.0	94.6	100.0	100.0	95.4
SR:SA=7:3	100.0	100.0	100.0	100.0	100.0	100.0	100.0	100.0	86.3	100.0	99.3	94.4
SR:SA=5:5	100.0	100.0	100.0	100.0	100.0	98.9	100.0	98.9	83.1	100.0	99.3	91.8
SR:SA=3:7	100.0	100.0	100.0	100.0	100.0	97.8	100.0	93.3	81.9	100.0	99.4	87.8
SR:SA=1:9	100.0	100.0	100.0	100.0	100.0	90.9	96.5	78.8	78.7	96.4	92.2	86.4
SA	61.0	54.6	45.6	72.4	75.7	79.2	76.2	75.4	78.0	74.5	78.4	82.0

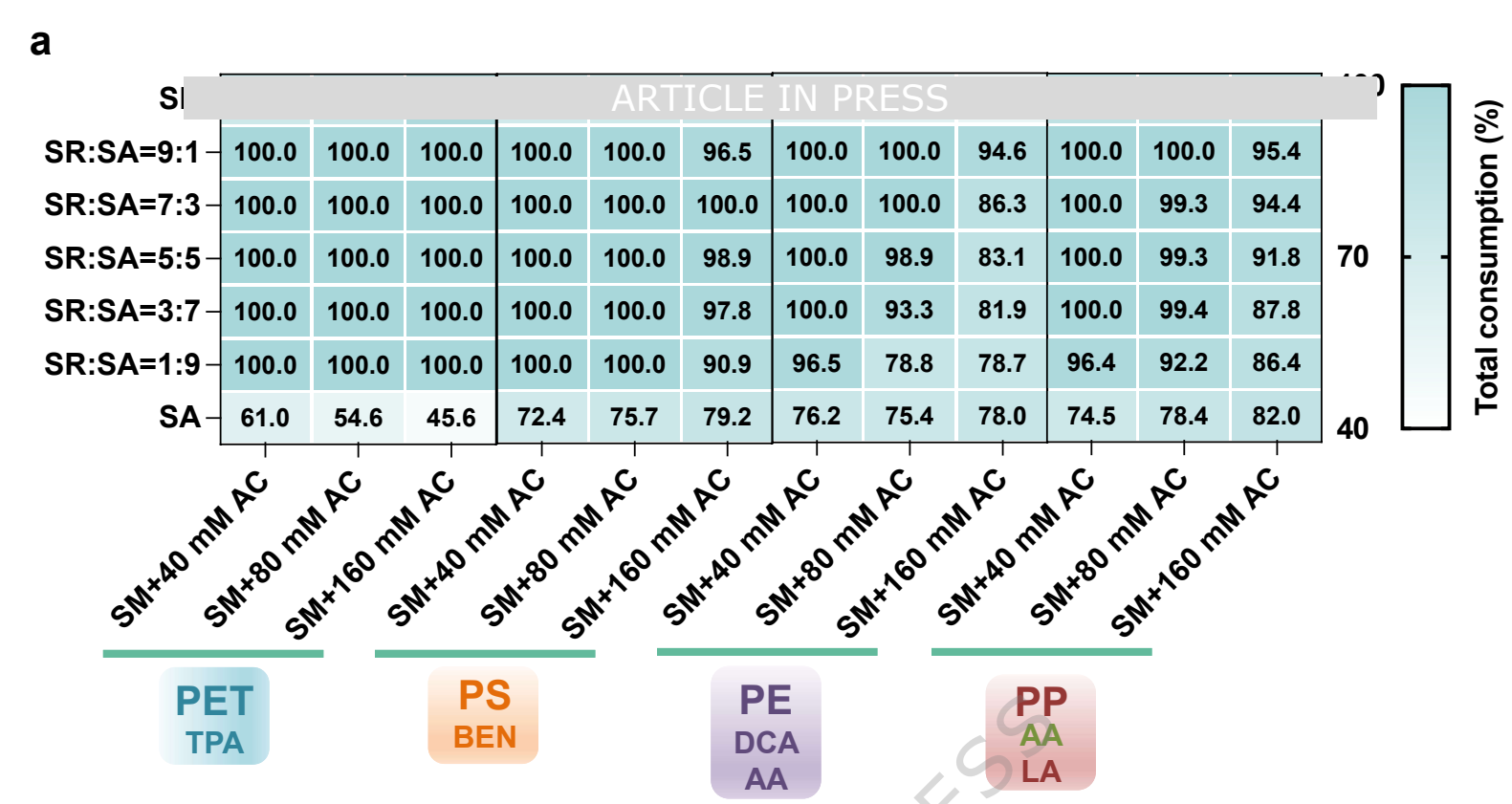

b

c

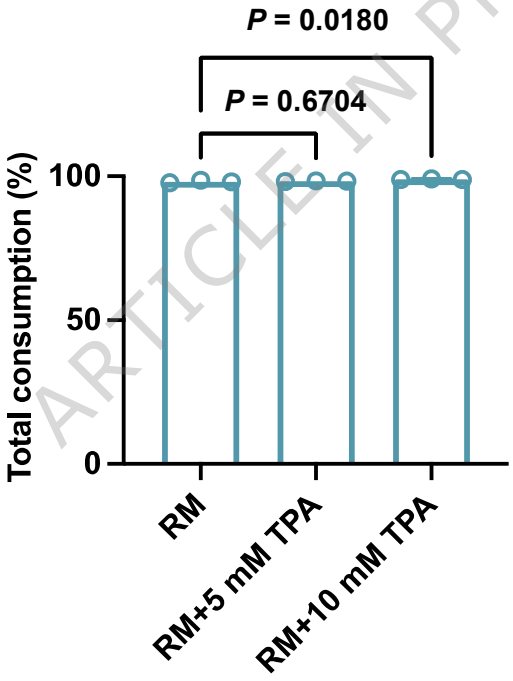

d